AD-A055 956 COLD REGIONS RESEARCH AND ENGINEERING LAB HANOVER N H F/G 20/14
INTERACTION OF A SURFACE WAVE WITH A DIELECTRIC SLAB DISCONTINU--ETC(U)
APR 78 S A ARCONE, A J DELANEY

UNCLASSIFIED CRREL-78-8 NL

1 OF 1
ADA
055956

END
DATE
FILMED
8-78
DDC

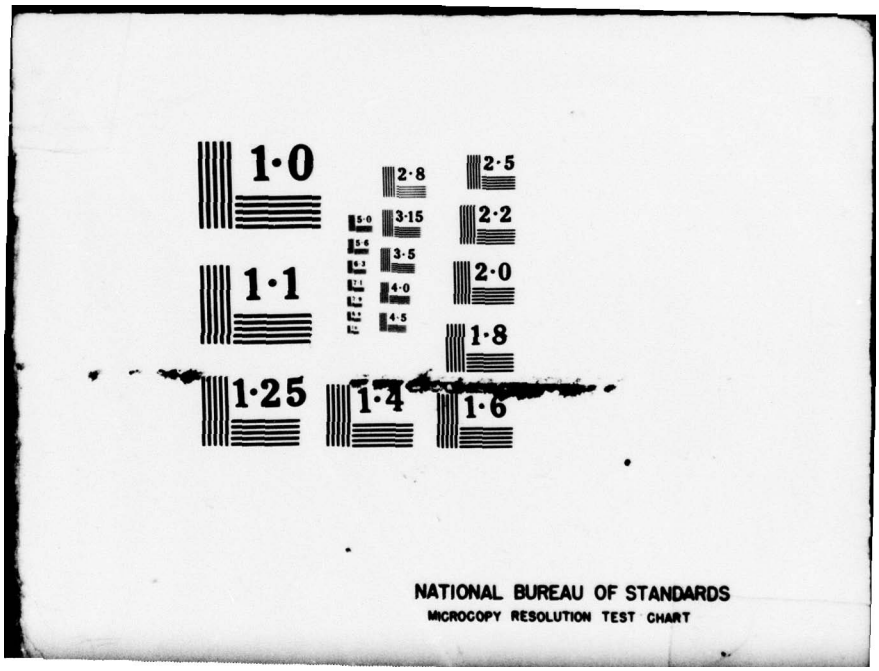
1·0
1·1
1·25
1·4
1·6
1·8
2·0
2·2
2·5
2·8
3·15
3·5
4·0
4·5
NATIONAL BUREAU OF STANDARDS
MICROCOPY RESOLUTION TEST CHART

CRREL REPORT 78-8

LEVEL II

12

Interaction of a surface wave with a dielectric slab discontinuity

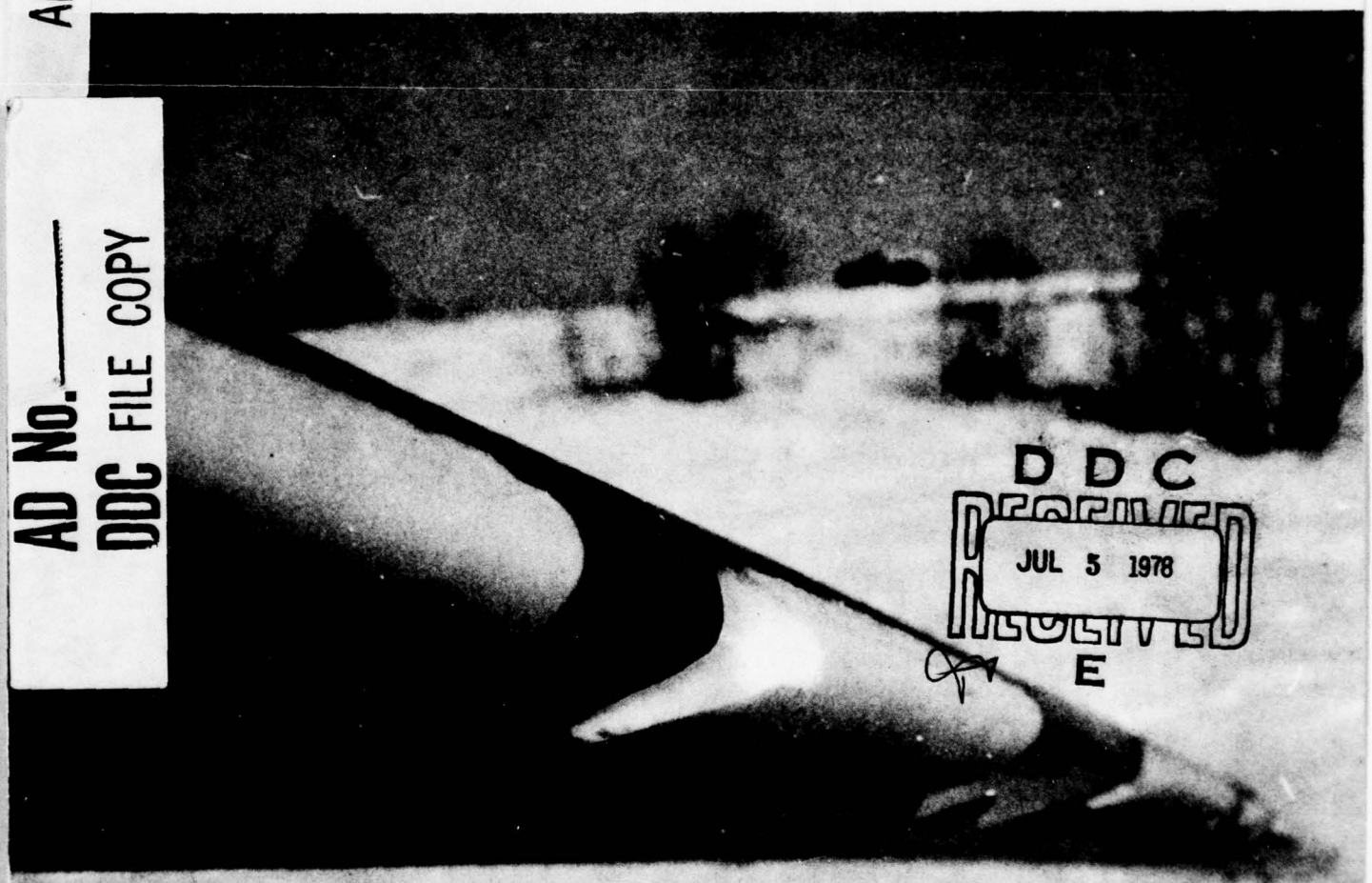

For conversion of SI metric units to U.S./British customary units of measurement consult ASTM Standard E380, Metric Practice Guide, *published by the American Society for Testing and Materials, 1916 Race St., Philadelphia, Pa. 19103.*

Cover: Ice accumulation on helicopter blade after winter flight. (Photograph courtesy of U.K. Aeroplane and Armament Experimental Establishment.)

CRREL Report 78-8

Interaction of a surface wave with a dielectric slab discontinuity

Steven A. Arcone and Allan J. Delaney

April 1978

Prepared for
DIRECTORATE OF MILITARY CONSTRUCTION
OFFICE, CHIEF OF ENGINEERS
By
CORPS OF ENGINEERS, U.S. ARMY
COLD REGIONS RESEARCH AND ENGINEERING LABORATORY
HANOVER, NEW HAMPSHIRE

Unclassified

SECURITY CLASSIFICATION OF THIS PAGE (When Data Entered)

REPORT DOCUMENTATION PAGE

READ INSTRUCTIONS BEFORE COMPLETING FORM

1. REPORT NUMBER: CRREL Report 78-8
2. GOVT ACCESSION NO.
3. RECIPIENT'S CATALOG NUMBER

4. TITLE (and Subtitle): INTERACTION OF A SURFACE WAVE WITH A DIELECTRIC SLAB DISCONTINUITY
5. TYPE OF REPORT & PERIOD COVERED
6. PERFORMING ORG. REPORT NUMBER

7. AUTHOR(s): Steven A. Arcone, Allan J. Delaney
8. CONTRACT OR GRANT NUMBER(s)

9. PERFORMING ORGANIZATION NAME AND ADDRESS: U.S. Army Cold Regions Research and Engineering Laboratory, Hanover, New Hampshire 03755
10. PROGRAM ELEMENT, PROJECT, TASK AREA & WORK UNIT NUMBERS: DA Project 4A161102AT24, Task A3E1, Work Unit 002

11. CONTROLLING OFFICE NAME AND ADDRESS: Directorate of Military Construction, Office, Chief of Engineers, Washington, D.C. 20314
12. REPORT DATE: April 1978
13. NUMBER OF PAGES: 16

14. MONITORING AGENCY NAME & ADDRESS (if different from Controlling Office)
15. SECURITY CLASS. (of this report): Unclassified
15a. DECLASSIFICATION/DOWNGRADING SCHEDULE

16. DISTRIBUTION STATEMENT (of this Report)

Approved for public release; distribution unlimited.

17. DISTRIBUTION STATEMENT (of the abstract entered in Block 20, if different from Report)

18. SUPPLEMENTARY NOTES

19. KEY WORDS (Continue on reverse side if necessary and identify by block number)

Airfoils
Deicing systems
Dielectric waveguides
Discontinuities
Microwaves

20. ABSTRACT (Continue on reverse side if necessary and identify by block number)

The interaction of a 5.1-GHz transverse electric surface wave with a dielectric slab is experimentally investigated. The wave is initially supported by a dielectric substrate resting upon a metallic ground-plane. A slab, made of the same dielectric material as the substrate and variable in height, is then placed upon the waveguide. The results for a small slab sitting on the substrate showed that the discontinuity was a very inefficient launcher of reflected surface waves. Investigations of these reflections with a trough waveguide showed that, for values of slab height comparable to the exponential decay height of the surface wave, the reflections remain very small. However, as the slab height is increased beyond the decay height, the reflected amplitude approaches the theoretical value for a plane wave reflected

next page

DD FORM 1 JAN 73 1473 EDITION OF 1 NOV 65 IS OBSOLETE

Unclassified

SECURITY CLASSIFICATION OF THIS PAGE (When Data Entered)

20. Abstract (cont'd)

from the interface between air and the same dielectric. The results are applicable to surface wave methods of microwave deicing of wings and helicopter rotors.

PREFACE

This report was prepared by Dr. Steven A. Arcone, Geophysicist, and Allan J. Delaney, Physical Sciences Technician, of the Physical Sciences Branch, Research Division, U.S. Army Cold Regions Research and Engineering Laboratory. The research described in this report was funded by DA Project 4A161102AT24, *Research in Snow, Ice and Frozen Ground*, Task A3, *Research in Terrain and Climatic Constants*, Scientific Effort E1, *Cold Environment Factors*, Work Unit 002, *Adhesion and Physics of Ice.*

The manuscript was technically reviewed by Dr. Kazuhiko Itagaki and L. David Minsk of CRREL.

The contents of this report are not to be used for advertising or promotional purposes. Citation of brand names does not constitute an official endorsement or approval of the use of such commercial products.

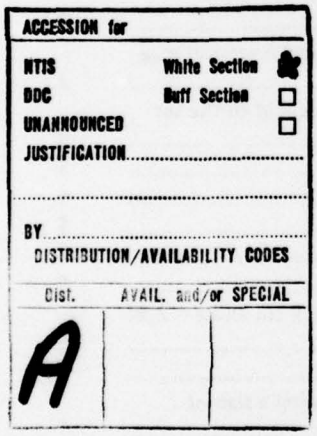

CONTENTS

ILLUSTRATIONS

TABLES

SUMMARY

A method of current interest in wing and helicopter rotor deicing is the application of microwave energy propagating along the leading edge of the airfoil in a surface wave mode. This mode can be established using a thin dielectric substrate or coating upon a metallic surface. The problem investigated experimentally in this report deals with the interaction of such a surface wave with a slab (or step) discontinuity resting upon a dielectric waveguide.

A piece of plexiglass of known dielectric constant was placed in a section of a rectangular waveguide which had one wall removed. The structure then supported a surface wave propagating at 5.1 GHz in the lowest order transverse electric mode. A short slab of the same dielectric constant was placed on the waveguide and the resulting disturbed electric field strength was recorded above the waveguide along its entire length. The field strength profiles revealed strong perturbations taking place at the forward and rear edges of the slab but a comparatively weak reflected wave from the slab. A further experiment was then conducted with a trough waveguide designed to guide most of the reflected energy in a surface mode. The results of this experiment showed that, for values of slab height comparable to the exponential decay height of the surface wave, the reflections are weak. As the slab height was increased, however, the reflected wave amplitude approached the theoretical value for plane wave reflection from a simple air dielectric interface. These studies suggest that surface waves propagating at microwave frequencies along rotors or wings may strongly couple into abrupt accumulations of ice.

INTERACTION OF A SURFACE WAVE WITH A DIELECTRIC SLAB DISCONTINUITY

Steven A. Arcone and Allan J. Delaney

INTRODUCTION

Background

The application of microwaves to the deicing of wings and rotors where ice rapidly accumulates on the leading edge of the airfoil (see cover) is of current interest. Pure ice is very absorptive (i.e. it has a high loss factor) in the electromagnetic spectrum below 100 kHz, but only a marginal loss factor exists at microwave wavelengths. However, if enough heat can be generated to cause a local melting, then deicing may accelerate due to the higher loss factor of liquid water in the microwave spectrum (1-100 GHz). Deicing may also result when the ice reaches approximately $-4^{\circ}C$, at which point the ice-substrate adhesion bond may weaken sufficiently to cause ice shedding.

The basic engineering problem of the design of a microwave airfoil deicing system is to generate and confine sufficient microwave energy in a manner that will not interfere with the mechanical requirements and aerodynamic design of the wing or rotor in question. Currently, consideration is being given to the use of the rotor or wing as a dielectric surface waveguide. A thin dielectric coating upon a metallic surface (e.g. rotor) is capable of confining propagating electromagnetic energy in a surface wave mode (so-called because the field strength decays with height above the guide) if the frequency, thickness and dielectric constant are properly chosen. Confined microwave radiation may then couple into an ice layer accumulating on the airfoil and cause the ice to shed as a result of internal dielectric heating.

The performance of a microwave deicing system is affected by the undesirable backscattering of a wave when inhomogeneities in the electrical properties of a material are encountered. The intensity of the scattering is determined by the size, shape and electrical parameters of the obstacle encountered and also the wavelength and nature (e.g. plane or spherical wave) of the incident radiation. In particular, the nature of a surface wave is such that the amplitude of the field strength varies exponentially along a plane of uniform phase situated perpendicularly to the direction of propagation. This nonuniformity presents a unique complication in the scattering process. In the ice adhesion application it is then necessary to investigate how such a wave will interact with an obstacle placed upon the waveguide. If the height of the obstacle is comparable or higher than the characteristic decay height, then one might expect severe reflections.

Objective and procedure

The objective of this research was to investigate the ability of a microwave surface wave to couple into a dielectric slab resting upon a uniform dielectric substrate. A plexiglass dielectric surface waveguide was designed and constructed to allow only the first order transverse electric mode surface wave to be propagated at 5.1 GHz. This wave mode was launched from within the dielectric waveguide. Plexiglass slabs of various heights were then placed on the waveguide. The surface wave electric field strength was measured along the entire length of the waveguide and slab. The results were used to estimate the amount of power lost by scattering from the slab discontinuity.

THEORY OF PLANE SURFACE WAVES

Surface waves have been extensively treated in the literature ever since Sommerfeld (1909) first established their theoretical basis. Subsequently, other investigators such as Norton (1936, 1937) refined the theory. These investigators intended their research to explain ground wave propagation at frequencies below about 10^7 Hz. With the advent of microwave technology in the 1940's, however, their results were also applied to laboratory surface waveguides. Much of this application has

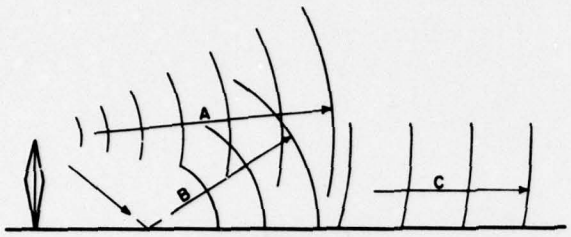

A Space Wave
B Reflected Wave
C Surface Wave

Figure 1. Various means of propagation from an antenna situated above a conducting or dielectric half-space.

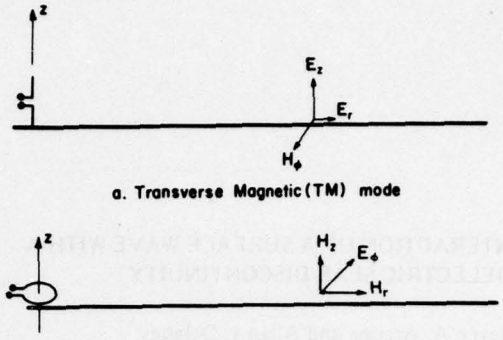

a. Transverse Magnetic (TM) mode

b. Transverse Electric (TE) mode

Figure 2. Wave propagation modes as generated by a vertical electric dipole (a) and a vertical magnetic dipole (b). z, r, and ϕ are cylindrical coordinates referenced to the dipole axes.

involved designing efficient surface wave launchers (Cullen 1954, Rich 1955, Cohn et al. 1960) because simple antennas placed above a conducting or dielectric surface will radiate most of their power into space. Investigations concerning the effect of inhomogeneities in the path of propagation have mainly been confined to flat surfaces containing discontinuities in electrical properties (Millington 1949, Wait 1956 and 1957, Feinberg 1959, King et al. 1973). Theoretical treatments of topographic irregularities have been given by Ott and Berry (1960) and Ott (1971), but experimental investigations of these irregularities have not been treated and are essentially the subject of this report.

The ensuing discussion briefly reviews the general features of plane surface wave transmission as described in Cartesian coordinates. Other coordinate geometries such as spheres and cylinders are also capable of supporting surface waves. Extensive treatises covering the theory of many surface waveguide possibilities may be found in the texts by Stratton (1941), Collin (1960), and Wait (1962).

Surface waves occur when an antenna is placed above or on the surface of some material, usually referred to as a half-space, of known dielectric permittivity, magnetic permeability and electrical conductivity. This situation is demonstrated in Figure 1. Three different means of radiation on and above the half-space then occur: 1) a direct space wave generated throughout the free space region, 2) an indirect reflected wave similarly generated throughout the free space region, and 3) a surface wave confined to the ground plane. At sufficient distance along the surface from the antenna, the space and reflected waves will cancel each other. This is due to the phase shift of 180° caused by the ground reflection when the indirect ray is incident upon the surface at a grazing angle of less than a few degrees. The only means of surface transmission is then the surface wave.*

Depending on the antenna type, transverse magnetic (TM) and/or transverse electric (TE) waves will be generated. This nomenclature refers to the field quantity that is exclusively orthogonal to the direction of wave propagation. These two types of wave modes are illustrated in Figure 2, where *E* refers to the electric field components and *H* to the magnetic field components. Simple electric and magnetic dipoles generate only the TM or TE modes, respectively, as shown in the figure, whereas more complex antennas such as arrays and horns may generate both mode types. It is also possible to generate both mode types by placing either an electrical (e.g. dielectric or conductive) or geometric discontinuity in the path of propagation.

Within the TM and TE mode classifications an infinite number of higher order modes can exist. When a dielectric coating is placed upon a metallic ground plane, however, the higher order surface wave modes may be suppressed upon selection of the proper signal frequency, permittivity, and thickness of the coating.

Since this investigation will be concerned with TE modes, only the mathematical formulation of these modes is presented. Equations for TM modes follow a similar development for which the reader is referred to the text by Collin (1960).

Using the coordinate system and waveguide parameters of Figure 3, the equations for the *E* and *H*

* Sometimes referred to as the "ground wave" in radio technology.

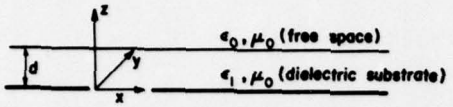

Figure 3. Coordinate reference system and waveguide parameters for development of the surface wave equations. d is the thickness of the substrate of dielectric permittivity ϵ.

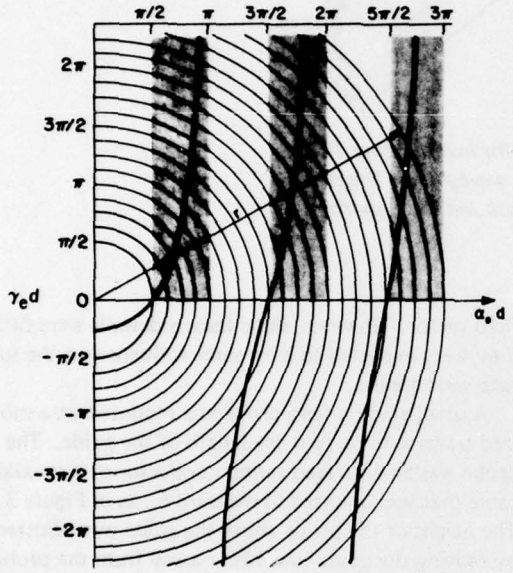

Figure 4. Graphical solution of the TE mode equations 7 and 8. Intersections of the curves within the shaded regions are permissible solutions allowing exponential decay away from the waveguide surface. Example: at a value $r = 11\pi/4$, three modes may propagate.

components of a TE wave propagating along the waveguide in a source free region are

$$E_{y0} = A_1 \, e^{-\gamma_e (z-d)} \, P \tag{1a}$$

$$H_{x0} = A_1 \, \frac{i\gamma_e}{\omega\mu_0} \, e^{-\gamma_e (z-d)} \, P \tag{1b}$$

$$H_{z0} = A_1 \, \frac{\beta_e}{\omega\mu_0} \, e^{-\gamma_e (z-d)} \, P \tag{1c}$$

for the upper air medium, and

$$E_{y1} = A_1 \csc(\alpha_e d) \sin(\alpha_e z) \, P \tag{2a}$$

$$H_{x1} = A_1 \, \frac{\alpha_e \csc(\alpha_e d)}{i\omega\mu_0} \cos(\alpha_e z) \, P \tag{2b}$$

$$H_{z1} = A_1 \, \frac{\beta_e \csc(\alpha_e d)}{\omega\mu_0} \sin(\alpha_e z) \, P \tag{2c}$$

where $P = e^{-i(\beta_e x - \omega t)}$ for the lower waveguide medium. A_1 is an arbitrary constant, ω the radian frequency (rad/s), t time in seconds, $i = \sqrt{-1}$ and $\mu_0 = 1.256 \times 10^{-6}$ H/m.

α_e and β_e are the wave propagation vectors in the z (standing wave) and x (traveling wave) directions, respectively, for the lower medium. γ_e and β_e are the traveling wave propagation vectors in the z and x directions, respectively, for the upper medium. They are interrelated by the equations

$$\omega^2 \mu_0 \epsilon_1 = \alpha_e^2 + \beta_e^2 \tag{3}$$

and

$$\omega^2 \mu_0 \epsilon_0 = -\gamma_e^2 + \beta_e^2 \tag{4}$$

where $\epsilon_1 = \kappa\epsilon_0$. κ is the relative permittivity, $\epsilon_0 = 8.85 \times 10^{-12}$ F/m, and α_e is determined from the transcendental equation

$$\alpha_e \cot(\alpha_e d) = -\sqrt{\omega^2 \mu_0 \epsilon_0 (\kappa - 1) - \alpha_e^2} \, . \tag{5}$$

The exponential decay factor γ_e is determined from α_e by the relation

$$\gamma_e = -\alpha_e \cot(\alpha_e d). \tag{6}$$

Equations 3-6 may now be used to obtain the following set of equations:

$$\gamma_e d = -\alpha_e d \cot(\alpha_e d) \tag{7}$$

$$(\gamma_e d)^2 + (\alpha_e d)^2 = (\kappa - 1)(\kappa_0 d)^2 \doteq r^2 \tag{8}$$

where $\kappa_0 = \omega\sqrt{\mu_0\epsilon_0}$ or $2\pi/\lambda$ where λ is the free space wavelength. These equations are graphed in Figure 4. The shaded regions represent permissible solution areas and each solution is defined by the intersection of the two curves. At a value $r = \pi/2$, $\gamma_e d$ becomes positive (thereby ensuring negative exponential growth above the waveguide) and the first order TE_1 mode is allowed. This mode is then permitted for all values of λ such that

$$\lambda < 4d\sqrt{\kappa - 1} \, . \tag{9}$$

When $r = 3\pi/2$, the TE_2 mode will also be excited; at $r = 5\pi/2$, the TE_3 mode, etc.

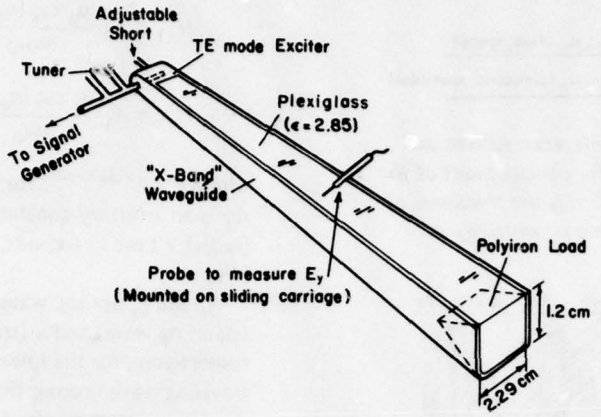

Figure 5. Experimental apparatus for investigating TE surface waves. The plexiglass fills the waveguide. The mode exciter is placed before the plexiglass and the polyiron load is inserted in it.

It must be remembered that the above theory applies to the ideal case of dielectric slabs that extend infinitely in the *xy* plane. However, when considering TE modes, perfectly conducting infinite waveguide walls may be inserted parallel to the *xz* plane without disturbing the fields. E_y is then terminated by an equivalent sheet of charge on the walls while H is terminated by an equivalent sheet of current. The use of such walls will then prohibit TE surface modes from losing field intensity due to spatial expansion of the wavefront when the modes are excited by a finite source.

WAVEGUIDE DESIGN AND CHARACTERISTICS

Physical apparatus

Figure 5 diagrams the equipment used for producing a TE_1 surface wave. A 114-cm plexiglass strip with a cross section of 2.29×1.02 cm was placed in a standard rectangular piece of waveguide with one narrow wall removed. The dielectric constant of the plexiglass was measured at 2.85 using standard waveguide techniques. A small exciter was inserted at one end of the waveguide before the plexiglass to excite the radiation and a polyiron wedge load was inserted in the plexiglass at the other end to absorb the radiation. A double-stub tuner was used to match the signal generator to the exciter. No attempt was made to maximize the efficiency of energy transfer into the surface wave mode, as only its propagation characteristics were to be investigated. Since radiation was in a TE mode, the mode characteristics would ideally be unaffected by infinite conducting sidewalls orthogonal to the electric field vector. However, since these sidewalls were finite, they were expected to have some influence on the surface wave fields.

A small electric field probe was mounted on a motorized traverse to carry it the length of the guide. The probe was an extended center conductor of a coaxial cable that was oriented to measure E_y as in Figure 3. The height of the probe above the guide was adjusted by moving the guide towards or away from the probe.

Frequency characteristics

According to Figure 4 propagation is possible at all frequencies above a cutoff frequency f_c determined by the relation

$$f_c = c/4d\sqrt{\kappa - 1}$$

where $c = 3\times10^{10}$ cm/s. Thus, for d = 2.29 cm and κ = 2.85, f_c = 2.41 GHz. Figure 6 shows the measured surface wave amplitude (in volts of recorder gain) as a function of frequency along with the voltage standing wave ratio (VSWR) as measured with a slotted line behind the double stub tuner. The tuner was used to achieve the best possible match at each frequency measured. The VSWR then determined the percentage of power reflected from the tuner. The strength of the surface wave was determined with the probe placed just before the load. Figure 6 shows that only minimal energy propagated below 3.2 GHz, while energy propagated at all frequencies above 3.2 GHz except at 6.8 GHz. At this latter frequency a severe mismatch occurred at the tuner which could not be alleviated.

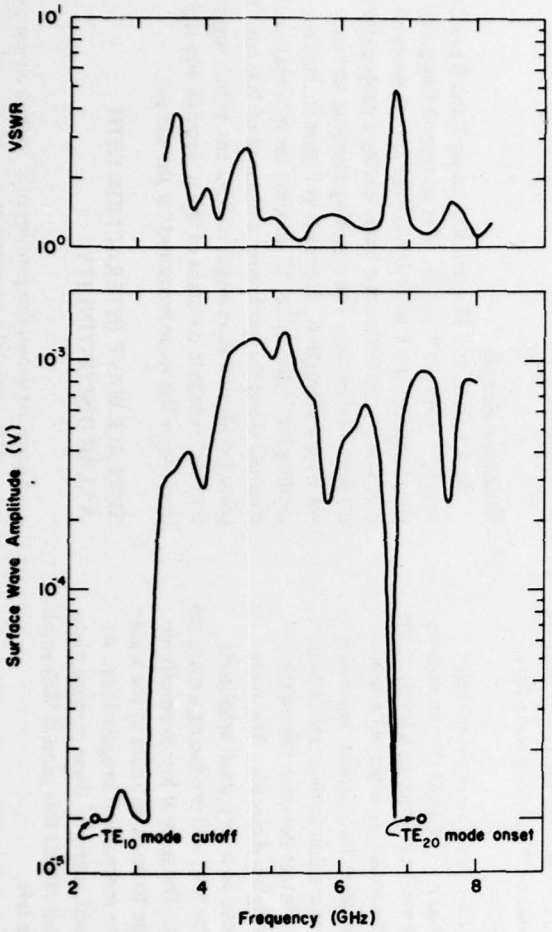

Figure 6. Frequency characteristics of the tuner-waveguide combination. No power could be measured below the theoretical cutoff frequency of 2.41 GHz. The minimal transmitted power at 6.8 GHz was due to a severe mismatch at the tuner.

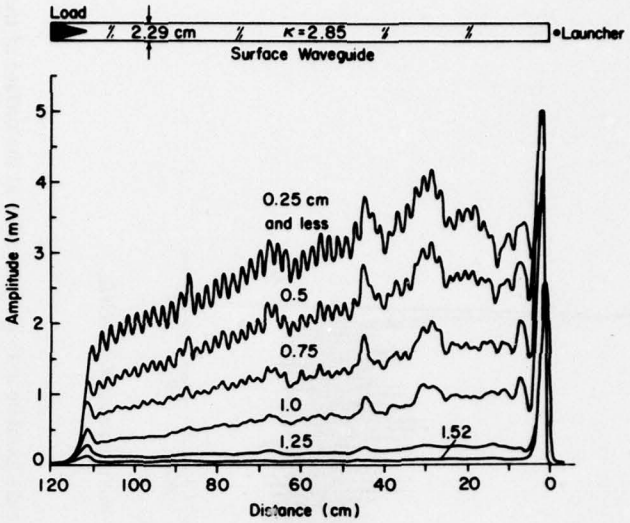

Figure 7. Profiles of E_y of the TE_1 surface wave at 5.1 GHz at various heights above the waveguide.

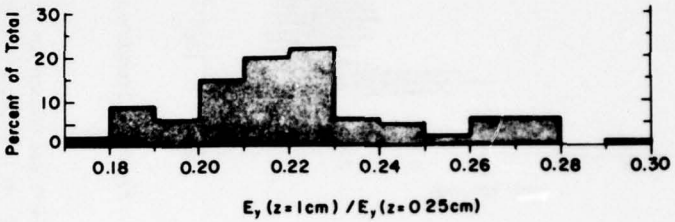

Figure 8. Normalized distribution of the ratio of the field strengths at z = 3.29 cm and z = 2.54 cm in Figure 8 for 100 positions along the waveguide.

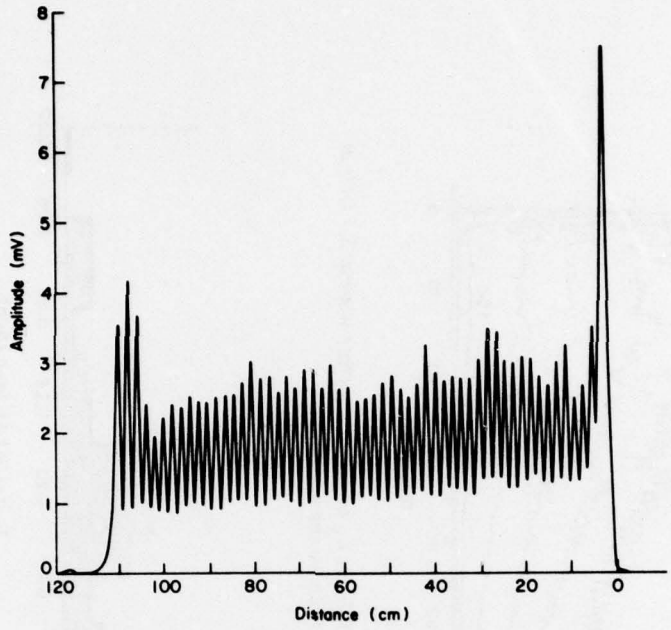

Figure 9. Standing wave pattern of the surface wave at 5.1 GHz.

A frequency of 5.1 GHz was chosen for study because of the low VSWR. At this frequency, no modes higher than the TE_1 were possible for the waveguide parameters used.

Spatial distribution of E_y above the guide

Ideally, a uniform traveling wave field that decays exponentially with height is desirable along the length of the guide. The actual amplitude (in mV of recorder gain) of the electric field of the surface wave that existed is shown in Figure 7.

Initially there is a sharp spike near the launcher where the dielectric begins. The field then maintains itself between 2 and 4 mV (amplifier gain level) at the 0.25-cm height until the load is reached, whereupon it rapidly decays. The larger fluctuations appearing about every 5 to 10 cm are due to mechanical imperfections such as poor contact between the metallic waveguide and the plexiglass dielectric. The more rapid oscillations are due to a very small amplitude wave reflected from the load and producing a marginal standing wave pattern. The general loss in amplitude from right to left is due to resistive losses in the walls and scattering from the mechanical irregularities. As probe height is increased, many of these perturbations persist and the field still retains this general 50% amplitude loss from right to left.

At 5.1 GHz, the first order solution of eq 7 and 8 predicts an exponential decay rate γ_e of 1.03 cm^{-1}. Therefore, at a height of 0.97 cm above the guide, the field should be at 0.37 of its value at the surface of the guide. Figure 8 gives the normalized distribution for the ratio of the field strengths at z = 2.54 cm and z = 3.29 cm heights as measured at 100 positions along the guide (variation in intensity from z = 2.54 cm to the guide surface was not measured). Fifty-seven percent of the values fall between 0.20 and 0.23, revealing a much more rapid decay than the theoretical value of $e^{-\gamma e}/e^{-0.25\gamma e} = 0.46$.

Guide wavelength

At 5.1 GHz, the TE_1 solution to eq 7 and 8 predicts that β_e = 1.49 cm^{-1} (eq 3). The corresponding guide wavelength in the x direction is 4.22 cm. A short circuit was placed before the load, leaving a propagation distance of 114 cm. The resulting standing surface wave field strength E_y is shown in Figure 9. Not including the initial spike, 52 maxima (or minima) can be counted along the guide over a distance of 100 cm. This corresponds to a wavelength of 3.92 cm, which suggests that the dielectric constant of the waveguide was slightly larger than the value measured for the sample.

SURFACE WAVE INTERACTION WITH A SLAB DISCONTINUITY

Figure 10 shows the profiles of E_y taken above the waveguide containing the slab discontinuity. The slab is made of the same plexiglass as the waveguide. The height of the probe above the waveguide (without the

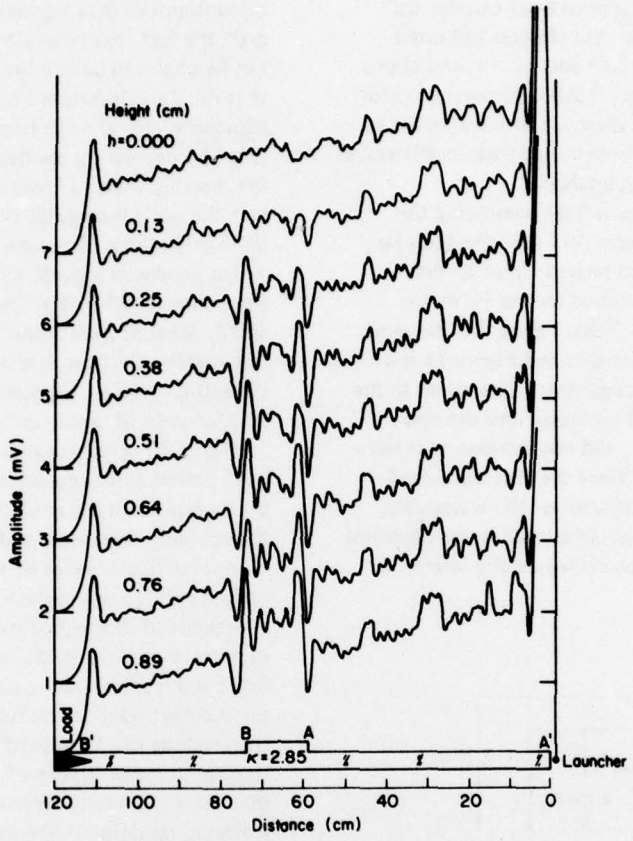

Figure 10. Profiles of electric field strength above a surface waveguide containing a slab of varying height h (see Fig. 11). The probe is at a fixed height of 1 cm above the surface of the basic waveguide. Frequency = 5.1 GHz.

slab) was fixed at 1 cm for all profiles and the length of the slab was fixed at 15 cm. In each successive profile going from top to bottom, the height h of the slab is increased by approximately 0.13 cm. Therefore, during this sequence the top of the slab moves closer to the fixed probe. The smallest vertical division represents 0.5 mV of recorder gain for the electric field strength.

Relative to the field trace at $h = 0$, the following observations may be made for the other traces:

1. The field over section A-A′ in all cases is nearly unchanged except for a slight modulation. Since 20 modulated cycles can be counted over a 40-cm section within A-A′, the modulation is a slight standing wave because $\lambda_g = 4.00$ cm.

2. Over section B-B′ all the field traces are nearly identical.

3. Over section A-B, the average field strength progressively increases with increasing h.

4. At point A there is a sharp decrease in field strength followed by a sharp increase to the left.

5. At point B there is a sharp increase followed by a sharp decrease to the left.

Points 4 and 5 can be elaborated upon by considering the simpler case of plane wave interaction for comparison. When a homogeneous plane wave of unit amplitude traveling in a semi-infinite medium of dielectric constant κ_1 is normally incident upon a semi-infinite medium of dielectric constant κ_2, the resulting electric field amplitude E at the interface is

$$E = \frac{2\sqrt{\kappa_1}}{\sqrt{\kappa_2} + \sqrt{\kappa_1}}$$

When $\kappa_2 > \kappa_1$, E is then less than 1 and the field strength has decreased. When $\kappa_2 < \kappa_1$, E is then greater than 1 and the field strength has increased.

Both these qualitative predictions hold true for the inhomogeneous plane wave field changes indicated above point A where $\kappa_2 = 2.85$ and $\kappa_1 = 1$, and above point B where $\kappa_2 = 1$ and $\kappa_1 = 2.85$. However, no further maxima or minima of these amplitudes persist to the right of these edges, demonstrating their inefficiencies as secondary surface wave launchers.

One can elaborate on point 3 by comparing the increases of field strength observed over the slabs (as they increased in height and moved closer to the probe) to the increases predicted by the TE mode solutions given previously. Table I gives the observed E_y values for varying slab heights and Figure 11 is a detail of the measuring arrangement. The values in the last column show that, as h increased and the slab moved nearer the probe, E_y did not increase as rapidly as theoretically expected. Since the slab was raised above the conducting lateral walls of the waveguide, it is probable that additional radiational losses occurred along the slab sides and thus decreased the observed field strength.

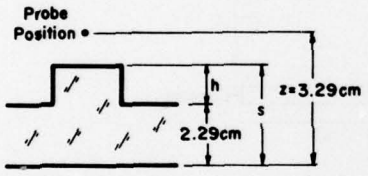

Figure 11. Probe position and slab dimensions for the data in Table I.

Table I. Comparison of theoretical and observed electric field strength ratios above the slab at $x = 68$ cm (see Fig. 10 and 11).

E_0 is the field strength when $h = 0.0$. The independent variable is h.

h (cm)	d (cm)	z-s (cm)	$E_y(z\text{-}s)/E_0$ Theoretical	Observed
0.0	2.29	1.00	1.00	1.00
0.13	2.42	0.87	1.12	1.00
0.25	2.54	0.75	1.24	1.06
0.38	2.67	0.62	1.41	1.10
0.51	2.80	0.49	1.59	1.13
0.64	2.93	0.36	1.71	1.23
0.76	3.05	0.24	1.88	1.24
0.89	3.18	0.11	2.06	1.29

EXPERIMENTS WITH A TROUGH

The above observations of increased field intensities at the slab edges (point A and B) suggested that these discontinuities may be causing large reflections. However, the fact that large standing wave patterns could not be observed before the discontinuities suggested that the discontinuities may be inefficient surface wave launchers. These reflections were then further investigated by decreasing the height of the dielectric below the metallic walls to form a trough. The extended metallic walls then guided the reflected surface waves more efficiently. The new value of d was 1.27 cm, which produced a guide wavelength of 5.51 cm at a frequency of 5.15 GHz (the theoretical values of γ_e and β_e are 0.332 cm^{-1} and 1.12 cm^{-1} respectively). The metal walls now extended 1.02 cm above the dielectric surface. The field traces (probe height = 2.34 cm) for slabs of two lengths are shown in Figure 12.

Figure 12 reveals that large standing waves existed both before and along the slabs, whereas E_y is practically unchanged from the case of $h = 0$ after the slab. Since the standing wave amplitude varies from cycle to cycle, no one particular value of VSWR can be assigned to each standing wave pattern. However, in Table II values are compiled of the maximum VSWR observed over each section of the guide for each value of h. Also listed is the approximate power in decibels lost from the incident wave to the reflected wave that the VSWR corresponds to. In spite of the apparently large standing wave patterns of Figure 12, the values in Table II show that there is actually very little power lost to back-scattered radiation in the xy plane. It is therefore assumed that free space losses above the trough waveguide are also negligible and that energy transfer to the slab is better than 90% efficient in all cases.

DISCUSSION AND CONCLUSIONS

It is helpful for analyzing the data of Table II to compute the VSWR that results when a homogeneous plane wave in free space reflects normally off a dielectric of relative permittivity κ. The VSWR is computed from the formula

$$\text{VSWR} = \frac{1 + |R|}{1 - |R|} \qquad (10)$$

where R, the reflection coefficient, is related to κ by

$$R = \frac{\sqrt{\kappa} - 1}{\sqrt{\kappa} + 1} . \qquad (11)$$

For a value of $\kappa = 2.85$, as was investigated above, the VSWR = 1.69. The value is approached by the maximum observed VSWR for the slab of Figure 12b. In the most severe case, $h = 0.95$ cm while γ_e^{-1} for the incident

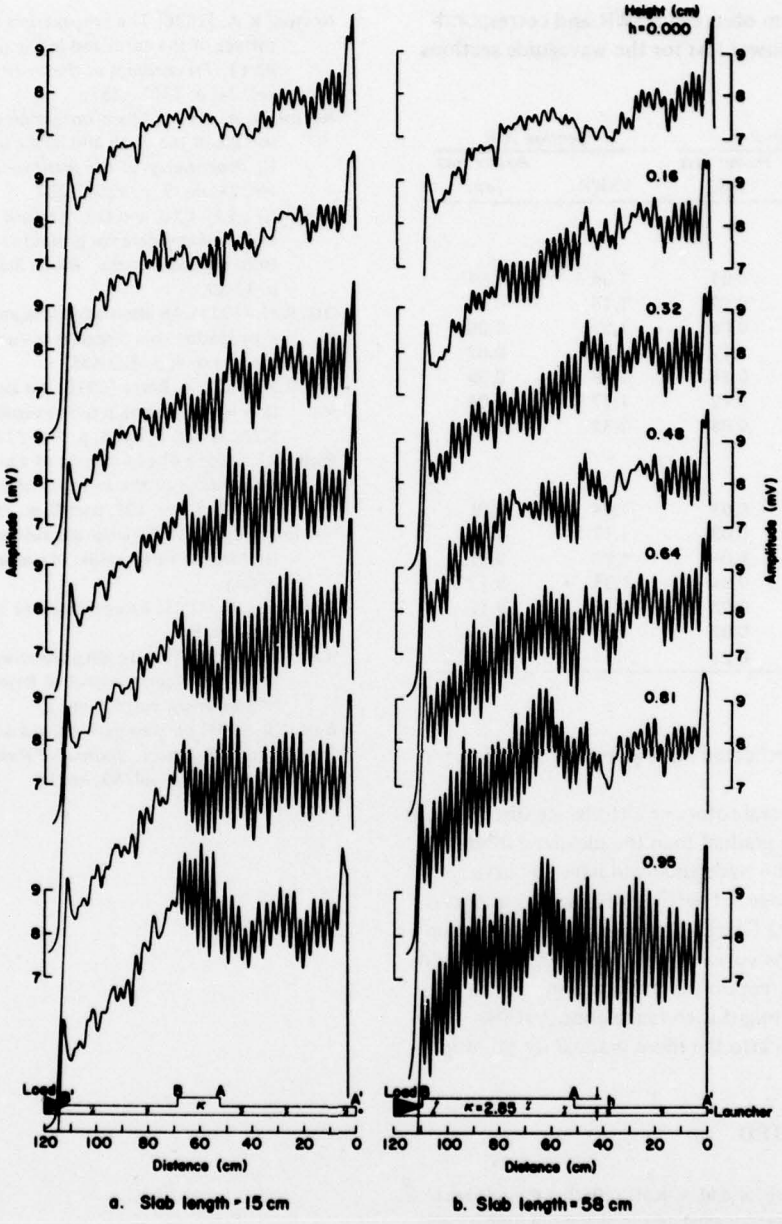

Figure 12. Profiles of electric field strength at 5.16 GHz above a dielectric trough waveguide containing two cases (a and b) of steps of height h but different lengths.

wave is computed at 3.01 cm for d = 1.27 cm. Therefore, the height of this discontinuity needed to be only 32% of the vertical exponential decay height of the field strength in order to produce reflections comparable to the more ideal (and assumed) case of homogeneous waves and infinite boundaries.

Since the dielectric constant of ice is 3.2, it is therefore reasonable to expect that the maximum VSWR possible would be 1.79 from any severe ice buildup. This would correspond to a maximum power loss for the incident surface wave of only 0.35 db. As demonstrated in the results, this power would then be

Table II. Maximum observed VSWR and corresponding approximate power loss for the waveguide sections of Figure 11.

h (cm)	Section A-A' VSWR	Section A-A' Power loss (db)	Section A-B VSWR	Section A-B Power loss (db)
Figure 12a				
0.00	1.10	0.03	1.04	0.01
0.16	1.08	0.02	1.18	0.04
0.32	1.26	0.08	1.25	0.08
0.48	1.36	0.12	1.23	0.07
0.64	1.43	0.16	1.29	0.09
0.81	1.37	0.12	1.17	0.04
0.95	1.25	0.08	1.32	0.10
Figure 12b				
0.00	1.10	0.03	1.04	0.01
0.16	1.11	0.03	1.17	0.04
0.32	1.20	0.05	1.23	0.07
0.48	1.15	0.04	1.35	0.12
0.64	1.25	0.08	1.36	0.12
0.81	1.24	0.07	1.54	0.21
0.95	1.56	0.22	1.51	0.20

very inefficiently reflected back along the surface waveguide.

For the case of real rotors or airfoils, ice distributions are of course more gradual than the idealized model chosen here, and the waveguide will have to curve around the rotor edge. If sufficiently high frequencies are used (such as 22 GHz) where free water absorption is maximal, then the curvature of the waveguide should have a negligible effect on the propagation. Surface microwave energy might then reach almost 100% coupling efficiency into the more gradual ice buildup.

LITERATURE CITED

Cohn, M., E.S. Cassedy, and M.A. Kott (1960) TE mode excitation on dielectric loaded parallel plane and trough waveguides. *Institute of Radio Engineering Transactions on Microwave Theory and Techniques*, p. 545-552, September.

Collin, R.E. (1960) *Field theory of guided waves*. New York: McGraw-Hill.

Cullen, A.L. (1954) The excitation of plane surface waves. *Proceedings of the Institute of Electrical Engineers* (London), vol. 101, part II, p. 225-234.

Feinberg, E.L. (1959) Propagation of radio waves along an inhomogeneous surface. *Bulletin of USSR Academy of Sciences*, supplement to vol. 9, series 1D, no. 1.

Millington, G. (1949) Ground wave propagation over an inhomogeneous smooth earth. *Proceedings of the Institute of Electrical Engineers* (London) vol. 96, part III, paper no. 794R.

Norton, K.A. (1936) The propagation of radio waves over the surface of the earth and in the upper atmosphere, Part I. *Proceedings of the Institute of Radio Engineers*, vol. 24, p. 1367-1387.

Norton, K.A. (1937) The propagation of radio waves over the surface of the earth and in the upper atmosphere, Part II. *Proceedings of the Institute of Radio Engineers*, vol. 25, no. 9, p. 1203-1237.

King, R.J., S.H. Cho, and D.L. Jaggard (1973)Height-gain experimental data for groundwave propagation. 2: Heterogeneous paths. *Radio Science*, vol. 8, no. 1, p. 17-22.

Ott, R.H. (1971) An alternative integral equation for propagation over irregular terrain, II. *Radio Science*, vol. 6, no. 4, p. 429-435.

Ott, R.H. and L.A. Berry (1970) An alternative integral equation for propagation over irregular terrain. *Radio Science*, vol. 5, no. 5, p. 767-771.

Rich, G.J. (1955) The launching of a plane surface wave. *Proceedings of the Institute of Electrical Engineers*, (London), vol. 102, part B, p. 237-246.

Sommerfeld, A. (1909) Über die ausbreitung der Wellen in der Drahtlosen Telegraphie. *Annalen der Physik*, vol. 28, p. 665.

Stratton, J.A. (1941) *Electromagnetic theory*. New York: McGraw-Hill.

Wait, J.R. (1956) Mixed-path ground wave propagation. 1: Short distances. *Journal of Research, National Bureau of Standards*, vol. 57, no. 1.

Wait, J.R. (1957) Mixed-path ground wave propagation. 2: Larger distances. *Journal of Research, National Bureau of Standards*, vol. 59, no. 1.

In accordance with letter from DAEN-RDC, DAEN-ASI dated 22 July 1977, Subject: Facsimile Catalog Cards for Laboratory Technical Publications, a facsimile catalog card in Library of Congress MARC format is reproduced below.

Arcone, Steven A.
Interaction of a surface wave with a dielectric slab discontinuity / by Steven A. Arcone and Allan J. Delaney. Hanover, N.H.: U.S. Army Cold Regions Research and Engineering Laboratory, 1978.
1 v, 16 p., illus; 27 cm. (CRREL Report 78-8.)
Prepared for Office, Chief of Engineers, under DA Project 4A161102AT24, U.S. Army Cold Regions Research and Engineering Laboratory.
Bibliography: p. 10.
1. Airfoils. 2. Deicing systems. 3. Dielectric waveguides. 4. Microwaves. I. Delaney, Allan J., joint author. II. U.S. Army. Corps of Engineers. (Series: U.S. Army Cold Regions Research and Engineering Laboratory, Hanover, N.H., CRREL Report 78-8.)